Transmitted power assessment from reverberant cavity set-up measurements

N. Schaefer[1,2], B. Bergen[1], B. Pluymers[2], W. Desmet[2]
[1] Toyota Motor Europe, Vehicle Performance Engineering Department, Noise and Vibration
B-1930 Zaventem, Belgium
e-mail: **nicolas.schaefer@toyota-europe.com**

[2] KU Leuven, Department of Mechanical Engineering
Celestijnenlaan 300 B, B-3001, Heverlee, Belgium

Abstract

This paper presents a novel method for the assessment of power radiated by a (treated) test panel. Conventional measurement techniques for panel radiation typically use either a diffuse field or a free-field as receiving environment. However, such an environment is not trivial to create, especially in a compact set-up. Therefore, a method is proposed to retrieve radiated power from a set of pressure measurements that can be applied in a small, reverberant receiving cavity. A base of modal shapes is used to describe the radiating panel velocity, complemented with a direct acoustic simulation of the receiving cavity. In this model, panel shape contribution factors are estimated from the pressure measurements. Finally, radiated power can be calculated from this model. For validation purpose, a bare plate case is considered, showing a good agreement between the original and reconstructed radiated power.

1 Introduction

Due to a continuous pursuit for lighter, more affordable and more silent cars, it has become a necessity to control the most accurately the vibro-acoustic performance of sound insulating packages, also called trim packages. This performance assessment has always been challenging for two main reasons: first, the difficulty of getting accurate measurements or numerical predictions; second, the gap between these data and the actual performance when applied inside the vehicle.

Typically, the performance of a trim package can be characterized by its acoustic absorption, structural damping, insertion loss and transmission loss. In this paper, focus is set on this latter one; transmission loss defined as

$$TL = 10\log\frac{W_{transmitted}}{W_{incident}} \tag{1}$$

Where $W_{incident}$ and $W_{transmitted}$ is respectively the incident power and the transmitted power on the panel.

Transmission loss measurements of flat trim samples can typically be done in coupled rooms, in impedance tube or in intermediate size set-ups. However, these different methods present some drawbacks. If coupled room measurements can accurately give the TL in the full-frequency range, it requires a lot of effort and big facilities. On the other hand, impedance tube measurements, by reducing to a very controlled environment, give measurements very sensitive to the boundary conditions [1]; finally, mid-size set-ups, such as Isokell [2] or “Small Cabin”, well-known within automotive industry, can only measure from a relatively high frequency limit. In these 3 kinds of set-ups, only airborne excitation is considered.

Moreover, the resulting transmission loss will differ when applied inside the vehicle. Indeed, first, the impedance of the vehicle will be different than the measurement condition (free or diffuse field); second, panels are also structurally excited on their boundaries by the skeleton of the car. In order to represent this kind of excitation in the problematic mid-frequency range, a set-up has been designed and validated [3, 4]. A clamped sample (350×500mm) is excited using a uniform boundary excitation, normal to the test panel, and backed by a reverberant cavity (550×700×800mm). The behaviour of the panel is captured thanks to 4 accelerometers on the plate and 6 microphones in the cavity. This set-up covers a wide frequency range of operation (100-1000 Hz), in which 8 uneven acoustic modes are present from 210Hz to 1 kHz. Indeed, due to the symmetry of the set-up excitation, only uneven cavity modes are excited.

This set-up, though closer to the vehicle application, presents the difficulty to retrieve the transmitted power compared to a diffuse or free-field condition. In order to retrieve this power, the velocity and pressure fields on the panel should be obtained first.

Many methods exist for reconstructing a source pressure and velocity fields from measurement data, such as holography, airborne source quantification or inverse methods.

Generalized and near field holography techniques [5, 6] are based on the analytic transformation to and from an appropriate eigenspace of pressure measurement. The field reconstitution is then based on an inverse back-propagation. These methods don't assume any prior knowledge of the environment (notably the shape of the radiating surface) and requires at least as many measurement points as desired reconstituted points, leading to a very fine measurement mesh and a low high-frequency limitation. An improvement to reduce the number of sensors is to use compressive sampling [7]. Additional difficulties arise when dealing with reverberant enclosed spaces [8].

Airborne Source Quantification (ASQ) [9] is based on estimation of strengths by inverse methods [10]. From the knowledge of the receiving geometry the pressure field can be quantified. Assuming the sources to be from a known pattern (monopole, dipole, patch), and exciting it separately, the method outputs transfer functions between receiver and source points. Then from an inverse-system solving the contribution of these different sources is estimated in order to fit the measured pressure field. A particularity of ASQ compared to inverse methods is the high numbers of microphones involved in order to get a good resolution for its typical applications (engine noise radiation, tyre noise, pass-by noise).

The method presented in this paper uses also an inverse problem solving, particularly suitable for a panel and cavity coupling. From measurements in a limited number of locations, the fields are recomposed from a base of shapes that are assumed to be the eigenshapes of the studied panel.

In the following sections, first the theoretical background of the method and its assumptions are presented. Finally the method is validated with a plate and cavity numerical model.

2 Method

This method is based on two sets of data:

- The operational data (subscripted $_m$) come from measurements in a limited number of points of the full system (panel and cavity). Commonly, those are pressure measurements from microphones.
- The shape model data come from simulation models containing only the cavity excited acoustically by one shape. These shapes derive from a known base; representative of the shapes that the panel would take on its resonance frequencies.
  For every shape i, a pressure field p_i and velocity field v_i are computed by simulation at every frequency.

The method considers that, at any frequency, the operational pressure field in $\boldsymbol{p_m}$ and velocity field $\boldsymbol{v_m}$ in the cavity are described as an expansion of the pressure fields $\boldsymbol{p_i}$ (respectively velocity fields $\boldsymbol{v_i}$) of panel excitation patterns:

$$\boldsymbol{p_m}(\omega) \approx \alpha_0(\omega)\boldsymbol{p_0}(\omega) + \sum_i \alpha_i(\omega)\boldsymbol{p_i}(\omega) \quad (2)$$

$$\boldsymbol{v_m}(\omega) \approx \alpha_0(\omega)\boldsymbol{v_0}(\omega) + \sum_i \alpha_i(\omega)\boldsymbol{v_i}(\omega)$$

where p_0 (respectively v_0) is the pressure field (respectively velocity field) in the cavity under the shape of the unit structural excitation; p_i (respectively v_i) is the pressure field (respectively velocity field) from the i^{th} shape model. The coefficients α_i are contribution factor of the different shapes and need to be determined at every frequency.

In Figure.1, a schematic representation of the method for a panel and cavity model is shown.

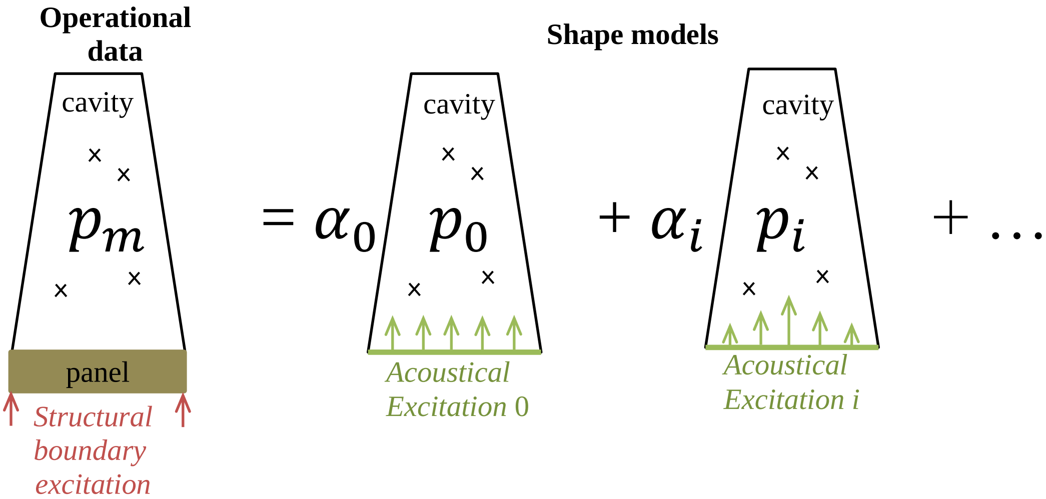

Figure.1: Schematic representation of the concept for pressure field;
example of a panel-cavity structurally excited on its boundaries

For sake of clarity, only pressure field is disserted hereafter as all velocity fields will follow the same relationship.

As the only input in the cavity is the acceleration of the panel, the recomposition made in (1) is accurate as long as the shape of the top surface of the panel can be written as a sum of the different shapes s_i.

A final and necessary step to include inside Equation (2) is the truncation of the field to a limited $n + 1$ number of shapes:

$$\boldsymbol{p_m}(\omega) \approx \alpha_0(\omega)\boldsymbol{p_0}(\omega) + \sum_{i=m(\omega)}^{m(\omega)+n(\omega)} \alpha_i(\omega)\boldsymbol{p_i}(\omega) \tag{3}$$

This truncation is needed in order to solve the contribution factors α_i from a limited number of measurements, by solving at every frequency the linear system

$$\begin{bmatrix} p_m(M_j) \\ v_m(M_j) \end{bmatrix} = \begin{bmatrix} p_0(M_j) & p_i(M_j) \\ v_0(M_j) & v_i(M_j) \end{bmatrix} \begin{bmatrix} \alpha_0 \\ \alpha_i \end{bmatrix} \tag{4}$$

This system can be solved for every frequency if the number of measurement points j is superior or equal to the number of shapes i, from least-square solving.

In this respect, first, the choice of microphone points is primordial, as they will condition the system written in equation (4). Various methods exist to optimize sensor positioning. A proposed method is to minimize the maximum value of the two second diagonal terms of the auto-MAC on pressure on the sensor points. Such a criterion will facilitate the differentiation for the shape association to resonance frequencies (see paragraph 3.4), which is key of the process.

Since the pressure field is expected to get its value from the contribution for a limited number of shapes j, an important process is to decide how to perform an optimal shape truncation over the whole frequency range. In order to choose the most contributing shapes, the method proposed in this paper is to calculate on every eigenfrequency the MAC of pressure on 8 microphones between the shape model data and the operational data.

3 Validation case

In this section, a validation case is presented, consisting of a clamped plate backed with a cavity. This layout is equivalent to the Toyota measurement set-up.

The base for the reconstitution consists in plate mode shapes. The field is reconstituted from 8 microphone measurements, which positions have been optimized.

In order to recompose the field, first resonance frequencies are identified, and then associated to a specific shape. Finally, field is recomposed on the resonance frequencies, compared to operational field, and then recomposed in-between resonance frequencies.

3.1 Model description

In order to simplify the computation, the validation model consists in a 1 mm-thick steel plate (500×700 mm) backed by a rectangular cavity (h = 550 mm). An impedance of 10^5 Pa.s/m is set on the cavity walls. This high impedance, representative of the cavity wall is the actual set-up, is needed to create power dissipation.

For sake of computation speed, this model has been reduced in an equivalent quarter model (250×350×550 mm).

Property	Value
Steel: Young Modulus	200 GPa
Steel: Loss Factor	0,2 %
Steel: Density	7600 kg/m³
Steel: Poison’s ratio	0.3
Air: Speed of Sound	346.15 m/s
Air: Density	1.2 kg/m³

Table 1: properties of steel and air used in the models

The first modes of this clamped plate are 20.5, 54.3, 92.4, 120, 123, 185, 215, 222, 252, 279, 312, 340, 403, 405, 410 and 440 Hz. All these modes are uneven, due to the symmetry of the excitation. The eigenfrequency information is not used during this procedure, only the eigenshapes are used as the shape base to recompose the field.

The first modes of the cavity are 314, 493, 584, 629 and 692 Hz. This modal base information is used in the procedure in order to exclude the cavity mode from the resonance frequency detection.

The frequencies studied in this validation case range from 210 to 409 Hz.

3.2 Choice of microphone points

The choice of microphone points was done by minimizing the maximum value of the two second diagonal terms of the auto-MAC on pressure on the sensor points. For this purpose the method developed by Carne and Dohmann [11] is used in order to re-calculate optimally the MAC at each iteration.

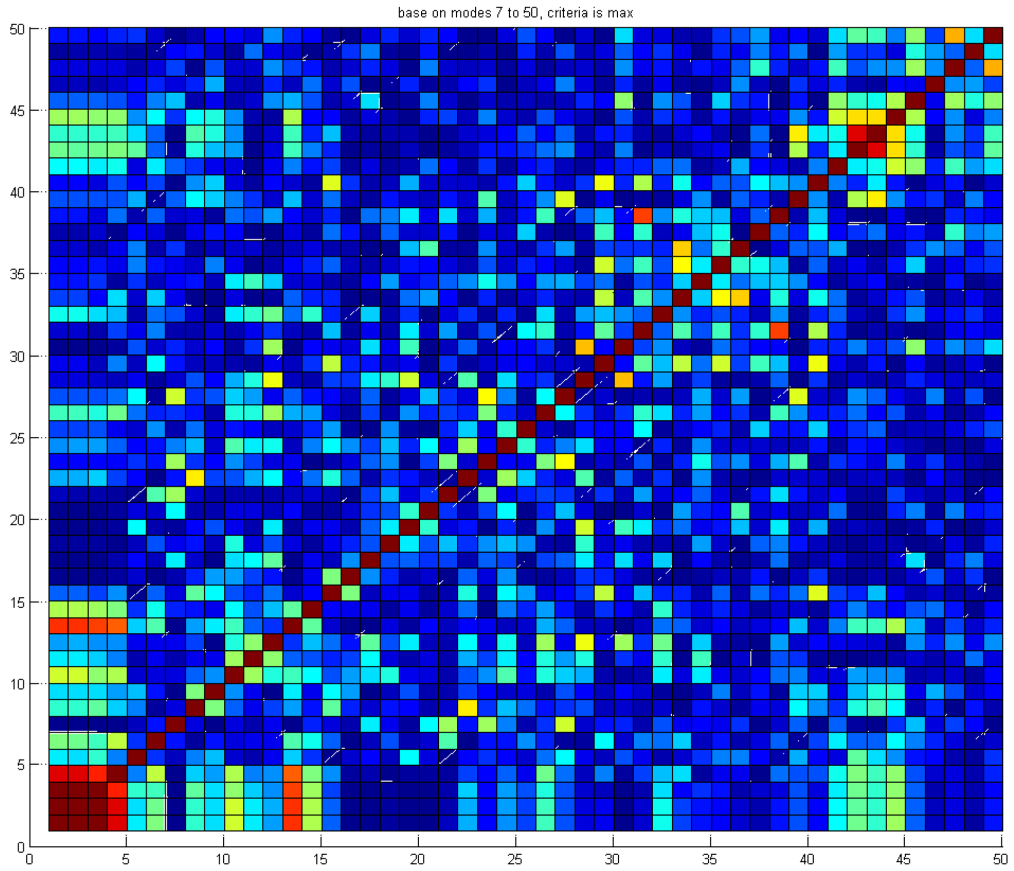

Figure.2: Resulting MAC from 8 microphones after optimization.

3.3 Coupled eigenfrequency detection

Resonance frequencies are detected based on the acceleration measurement from the plate. In Figure.3 the acceleration in a point of the plate is plotted. The resonance frequencies kept are 215, 221, 252, 278, 311, 341 and 404 Hz.

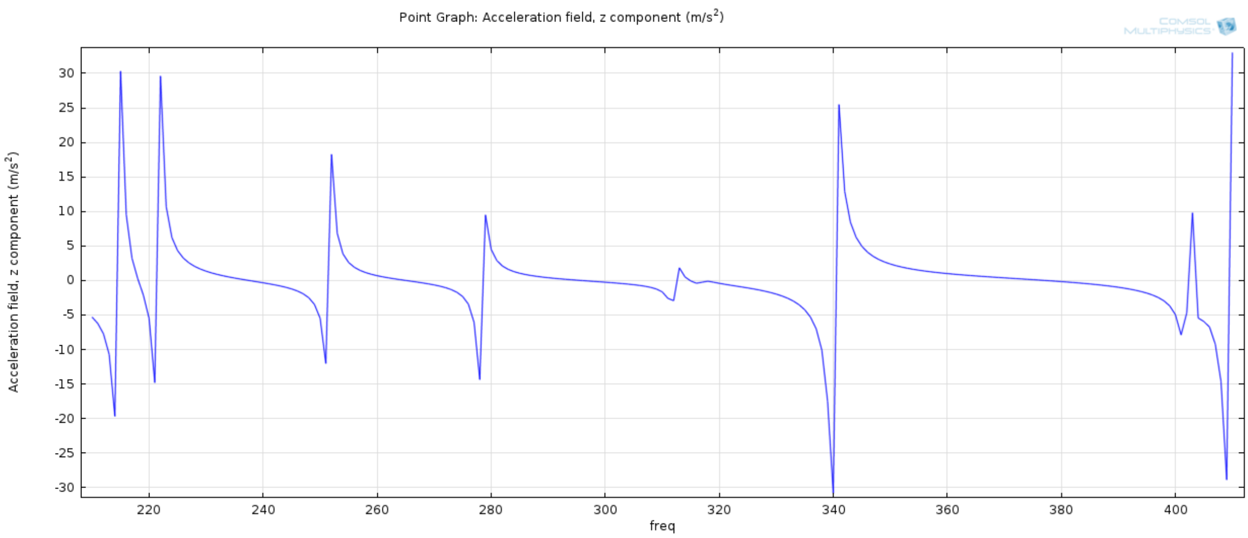

Figure.3: Acceleration measurement on the plate

This process can be automated by considering algorithms used in experimental modal analysis to detect eigenfrequencies.

3.4 Shape association

In order to associate a shape, first the shapes are computed from modal analysis of a clamped plate.

For each of those resonance frequencies, the MAC on pressure between operational and shape models on the 8 microphones is checked. This allows to associate every resonance frequencies to a specific shape k.

$$MAC_{ij} = \frac{|p_m \overline{p_i}|^2}{p_m \overline{p_m} p_i \overline{p_i}} \tag{5}$$

Where $\overline{}$ is the complex transpose function, p_m and p_i are the pressure from operational data (respectively from the shape model i) on the 8 measurement points at the frequency ω_j.

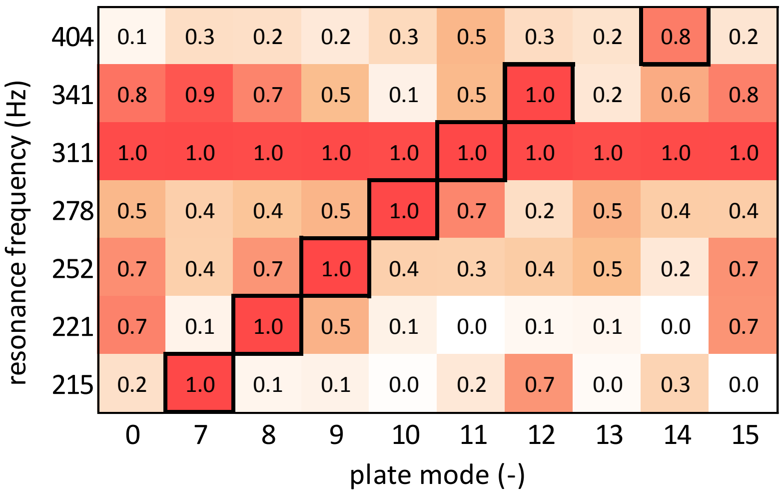

Figure.4: MAC between operational and shape models on microphone on resonant frequencies

2 problems can be underlined in the MAC association done in Figure.4:

- For the resonance frequency 311 Hz, all the MAC = 1. This occurs because of the cavity mode at 315 Hz, which gives a similar pressure field whatever the excitation is. In this respect, the clamped plate mode at 312 Hz, corresponding to the mode shape 11 couldn't be distinguished. In order to tackle this issue, the cavity modal analysis with its frequencies should be included in this process.
- For the shape number 13, no resonance frequency has been selected. This is due to its proximity in frequency to shape 14 (402 and 405 Hz), and therefore was not detected during the previous step. In order to tackle this issue, this process should also consider the frequency around the peaks. In the Figure.5, the MAC is calculated for resonance frequency ± 2Hz, and this shape 13 is finally associated.

These 2 improvements are not considered in the following steps.

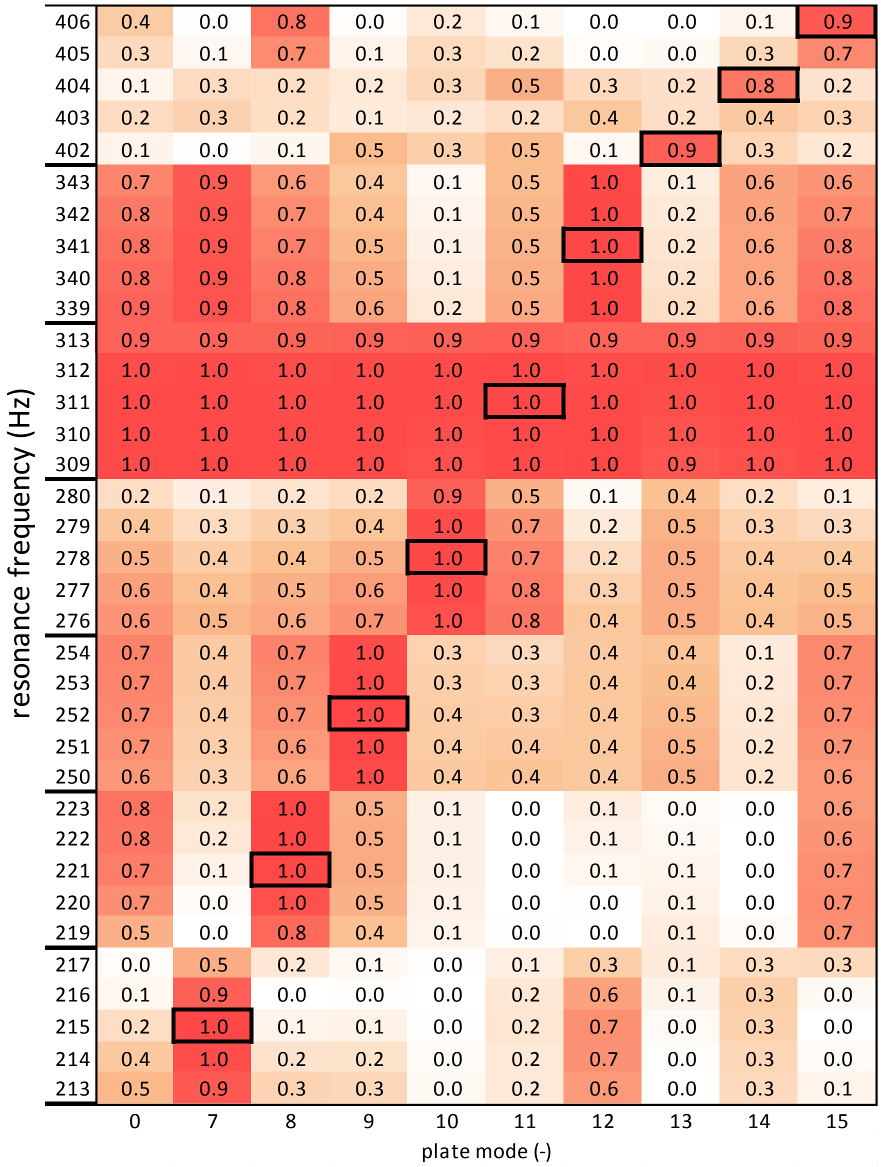

Figure.5: MAC between operational and shape models on microphone around resonance frequencies

3.5 Reconstruction on the resonance frequencies

Based on the 8 microphones, the operational field at every resonance frequency is reconstructed only from the unit acceleration mode and the shape found in the previous step, at the same frequency.

It has to be noted that the choice of only using one shape mode in addition to the excitation mode to reconstruct the field is arbitrary and can be improved base on the MAC value obtained in the previous step. Indeed, as underlined before, for the modes 13 and 14, close in frequency it should give a better approximation due to the probable coupling of the modes.

$$p_{ope}(\omega_k) = \alpha_0(\omega_k)p_0(\omega_k) + \alpha_k p_k(\omega_k) \quad (6)$$

In the Figure.6 and Figure.7, the reconstructed pressure field (respectively velocity field) is plot against the actual operational field for the 215Hz resonance (which has a very good MAC). Absolute error is also plotted on the same scale. It shows a very good agreement.

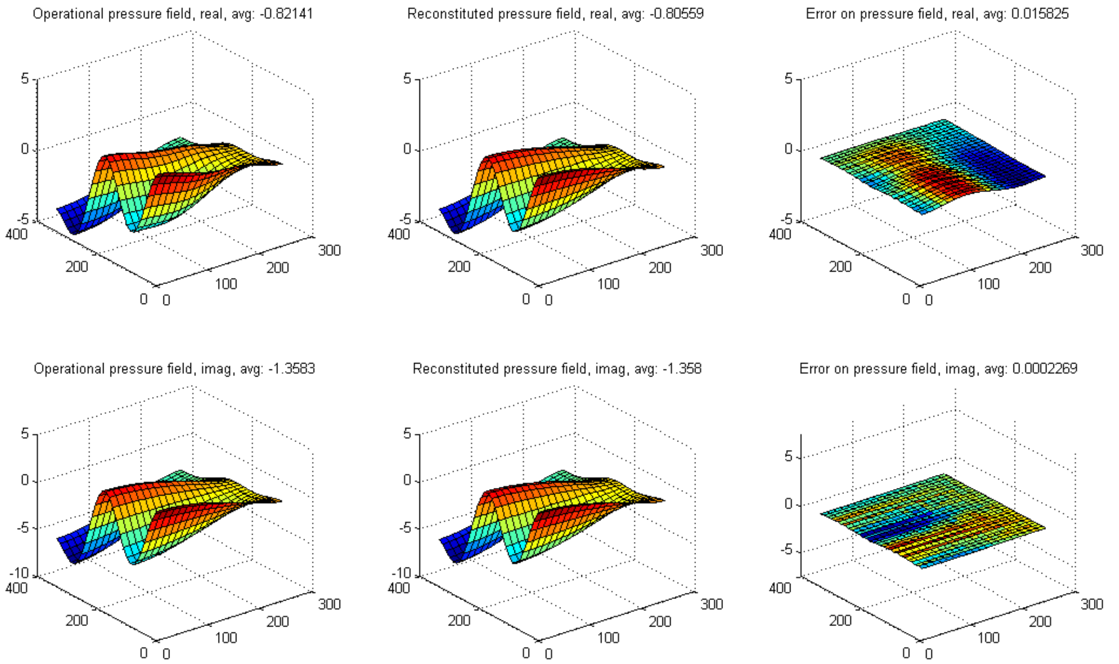

Figure.6: operational (left) against reconstituted (middle) pressure fields and error (right) for 215 Hz

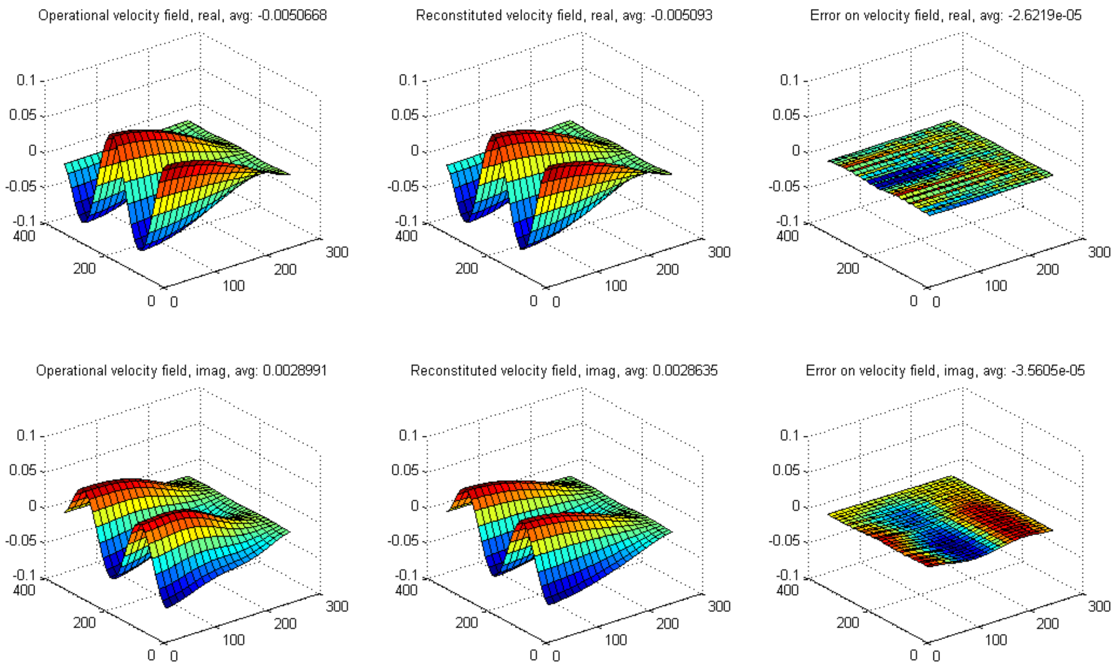

Figure.7: operational (left) against reconstituted (middle) velocity fields and error (right) for 215 Hz

3.6 Reconstruction in-between the resonance frequencies

Finally, between every set of two resonance frequencies, the operational field has been reconstructed from the unit acceleration mode and the shapes of a number *n* of surrounding modes, as written in Equation (3)

In order to validate the recomposition, Figure.8 shows the reconstituted transmitted power on the top surface of the plate against the operational power for the cases of reconstruction with 2 and 4 modes.

The transmitted power is calculated as:

$$TP = \frac{1}{2}\mathrm{Re}\left(\iint_{S_{panel}} pv^{*}dS\right) \quad (7)$$

Again, this shows good agreement. The mismatch is observed in the frequency range from 350 to 400 Hz comes from the wrong shape association, as already underlined in paragraph 3.4.

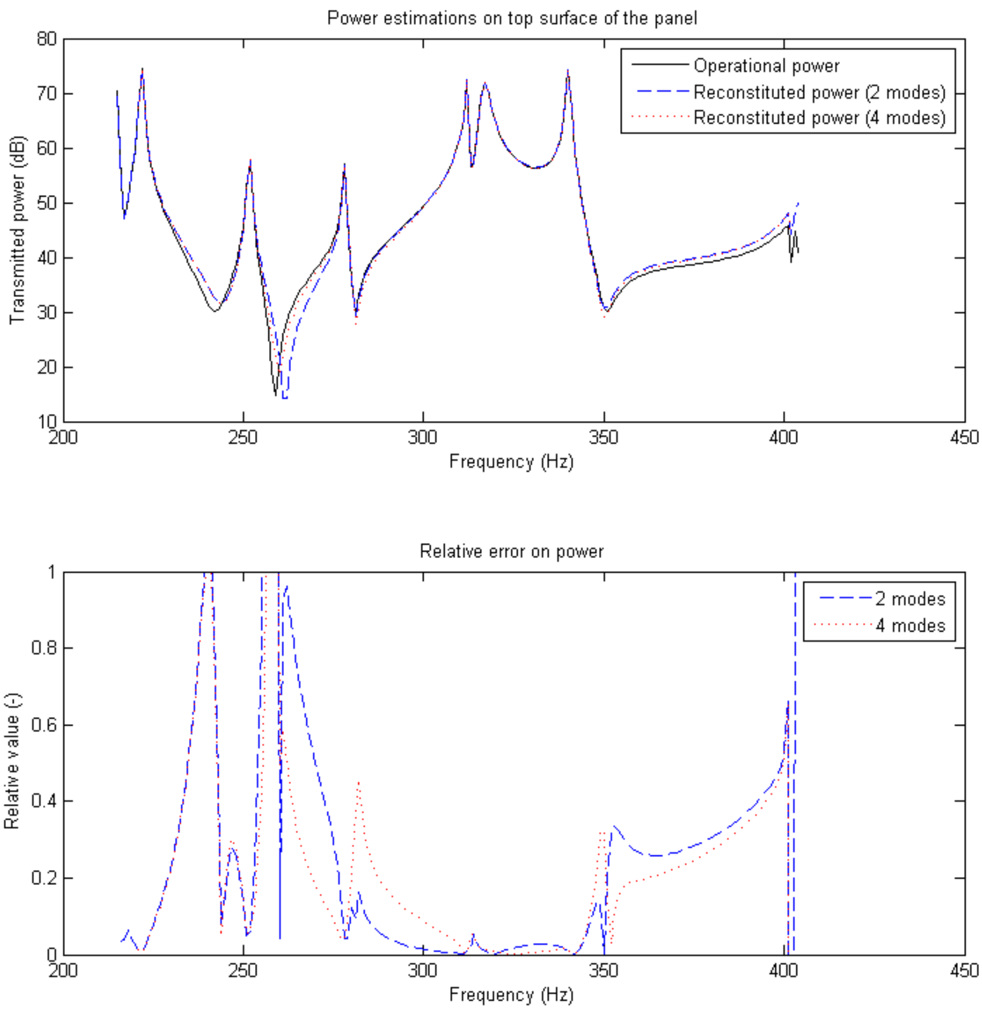

Figure.8: Power estimation for operational and reconstituted power (top), relative error (bottom)

4 Conclusions and future work

A new method to predict velocity and pressure fields, based on the prior knowledge of the panel modal shapes, has been presented. The method has been validated with a numerical plate and cavity model with good agreement over the frequency range.

Still, during the validation, improvements of the method for this specific case have been underlined. During shape association process (3.4),

- the prior knowledge of the modal behavior of the cavity can be included in the model to increase accuracy.
- the consideration of the potential coupling of different panel shapes on the same resonance frequency can be tackled by combining different modes.

Moreover, for highly damped panels, the detection process of eigenfrequencies of the coupled panel (0) could be less accurate. As an improvement, the shape association process could be used for both finding eigenfrequencies and eigenshapes.

Finally, when modal density is too high, the method should break down, due to the difficulty to associate a shape:

- As an alternative the field could be spatially sub-structured in different patches excited with a unit acceleration pattern instead of mode shapes and the same method could be applied.
- If the field could be considered as diffuse, the power is estimated from p_m^2.

Acknowledgements

The authors would like to gratefully acknowledge institute for promotion of science in Flanders (IWT) for their support.

Norimasa Kobayashi and Hiroo Yamaoka from Toyota Motor Corporation, Japan, are gratefully acknowledged for their technical support.

References

[1] K. V. Horoshenkov, A. Khan, *Reproducibility experiments on measuring acoustical properties of rigid-frame porous media (round-robin tests)*, J. Acoust. Soc. Am., Vol. 122 (2007), pp. 345-353.

[2] A. Chappuis, *Small-size device for accurate acoustical measurements of materials and parts used in automobiles*, SAE Technical Papers 931266, *Proceeding of the 1993 noise and Vibration conference*, p. 264.

[3] M. Vivolo, B. Pluymers, B. Van Genechten, D. Vandepitte, W. Desmet, *Study of the vibro-acoustic behaviour of composite sandwich structures by means of a novel test setup*, *Proceedings of ISMA2012*, Leuven, Belgium, 2012 September 17-19, Leuven (2012).

[4] C. Van der Kelen, M. Vivolo, B. Van Genechten, B. Pluymers, W. Desmet, A. Malkoun, B. Bergen, T. Keppens, *Validation of a dedicated test set-up for boundary excitation of trim assemblies*, *Proceedings of ISMA2012*, Leuven, Belgium, 2012 September 17-19, Leuven (2012).

[5] J. D. Maynard, E. G. Williams, Y. Lee, *Near-field acoustic holography: I. Theory of generalized holography and the development of NAH*, J. Acoust. Soc. Am., Vol. 78(1985), pp. 1395–1413.

[6] W.A. Veronesi, J. D. Maynard, *Digital holographic reconstruction of sources with arbitrarily shaped surfaces*, J. Acoust. Soc. Am., Vol. 85 (1989), pp. 588–598.

[7] G. Chardon, L. Daudet, A. Peillot, F. Ollivier, N. Bertin, R. Gribonval, *Near-field acoustic holography using sparse regularization and compressive sampling principles*, J. Acoust. Soc. Am., Vol. 132 (2012), pp. 1521-1534.

[8] D. Berckmans, P. Kindt, P. Sas, W. Desmet, *Evaluation of substitution monopole models for tire noise sound synthesis*, Mechanical Systems and Signal Processing, Vol. 24, No.1 (2010), pp.240-255.

[9] G. Verenosi, C. Albert, E. Nijman, J. Rejlek, A. Bocquillet, *Patch transfer function approach for analysis of coupled vibro-acoustic problems involving porous materials*, SAE Technical Paper 2014-01-2092 (2014).

[10] P. A. Nelson, S.H. Yoon, *Estimation of Acoustic Source Strength by Inverse Methods*, *Part 1, Conditioning of the inverse Problem*, Journal of Sound and Vibration, Vol. 233, No. 4 (2000), pp.643-668.

[11] T. Carne, C. Dohmann, *A modal test design strategy for modal correlation*. *Proceedings of the 13th International Modal Analysis Conference* (1995), pp. 927-933.